PANNEXIN-1 CHANNEL REGULATES NUCLEAR CONTENT PACKAGING INTO APOPTOTIC BODIES AND THEIR SIZE

Thanh Kha Phan[1*#], Pamali Fonseka[1*], Rochelle Tixeira[2], Mohashin Pathan[1], Ching-Seng Ang[3], Dilara Ceyda Ozkocak[1], Suresh Mathivanan[1#], Ivan Ka Ho Poon[1#]

[1]Department of Biochemistry and Genetics, La Trobe Institute for Molecular Science, La Trobe University, Melbourne, Victoria 3086, Australia

[2]VIB-UGent Center for Inflammation Research, Department of Biomedical Molecular Biology, Ghent University, Ghent, Belgium

[3]The Bio21 Molecular Science and Biotechnology Institute, University of Melbourne, Parkville, Victoria 3010, Australia

[#] Corresponding author: Thanh.Phan@latrobe.edu.au (T.K.P.), S.Mathivanan@latrobe.edu.au (S.M.), I.Poon@latrobe.edu.au (I.K.H.P.)

[*]T.K.P. and P.F. contributed equally to this work

List of abbreviations

ApoBDs: apoptotic bodies, EV: extracellular vesicle, PANX1: pannexin 1, HMGA1: high mobility group protein A1, THYN1: thymocyte nuclear protein 1, NUP50: 50 kD nucleoporin, GO: gene ontology.

Keywords

Apoptotic bodies, extracellular vesicles, pannexin 1, cargo sorting, nuclear proteins, DNA

Word count (including references as well as figure and table legends): 5,246

Abstract

Apoptotic bodies (ApoBDs), which are large extracullular vesicles exclusively released by apoptotic cells, possess therapeutically exploitable properties including biomolecule loadability and transferability. However, current limited understanding of ApoBD biology has hindered its exploration for clinical use. Particularly, as ApoBD-accompanying cargoes (*e.g.,* nucleic acids and proteins) have major influence on their functionality, further insights into the mechanism of biomolecule sorting into ApoBDs are critical to unleash their therapeutic potential. Previous studies suggested pannexin 1 (PANX1) channel, a negative regulator of ApoBD biogenesis, can modify synaptic vesicle contents. We also reported trovafloxacin (a PANX1 inhibitor) increasing proportion of ApoBDs containing DNA. Therefore, we sought to define the role of PANX1 in regulating the sorting of nuclear content into ApoBDs. Here, using flow cytometry and label-free quantitative proteomic analyses, we showed that targeting PANX1 activity during apoptosis, via either pharmacological inhibition or genetic disruption, resulted in enrichment of both DNA and nuclear proteins in ApoBDs that were unexpectedly smaller in size. Our data suggest that PANX1, besides being a key regulator of ApoBD formation, also functions as a negative regulator of nuclear content packaging and modulator of ApoBD size. Together, our findings provide further insights into ApoBD biology and form a novel conceptual framework for ApoBD-based therapies through pharmacologically manipulating ApoBD contents.

Statement of significance

Unleashing the therapeutic potential of apoptotic bodies (ApoBDs) requires an advanced understanding in ApoBD biogenesis, particularly mechanisms underlying ApoBD cargo packaging. Our findings presented herein uncovers a novel role of PANX1, a known regulator of ApoBD formation, in negatively regulating the sorting of nuclear proteins into ApoBDs and influencing their size. Significantly, our findings not only provide further insights into ApoBD biology but also offer an unprecedented approach to pharmacologically manipulate contents in ApoBDs for ApoBD-based therapies using PANX1 inhibitors.

1. Introduction

Apoptosis (a form of programmed cell death) occurs as a vital part of homeostasis and physiopathology such as chronic inflammation and infection [1,2]. Cells undergoing apoptosis often release apoptotic bodies (ApoBDs), a distinct type of membrane-bound extracellular vesicles (EVs) generally considered as 1−5 μm in size, to communicate with other cells to regulate cell clearance, tissue repair and/or immune response [3]. Recently, in contrast to previously thought, ApoBD formation is a highly co-ordinated process known as apoptotic cell disassembly consisting of three morphological steps: (i) membrane blebbing, (ii) thin membrane protrusions (*e.g.* apoptopodia), and (iii) fragmentation to form discrete ApoBDs. Firstly, coordinated by several protein kinases in particular caspase-activated Rho-associated kinase 1 (ROCK1), apoptotic cells form membrane blebs on the cell surface [4–6]. The dying cells' membrane then extends, resulting in long membrane protrusions to radiate the blebs. This step is typically negatively regulated by the caspase-activated membrane channel pannexin 1 (PANX1) and, in certain cell types (*e.g.* monocytes), positively controlled by the caspase-cleaved membrane receptor plexin B2 (PLXB2) [1,7]. Afterwards, numerous ApoBDs are released through the fragmentation of the membrane protrusions and/or apoptotic cells [8].

Despite current modest knowledge of ApoBD functions, it is becoming clear that ApoBDs also possess a few similar therapeutically exploitable properties compared to other EV subtypes [3]. Particularly, ApoBDs are readily available and easily purified from bodily fluids [9,10]. ApoBDs can also facilitate intercellular communication through biomolecule trafficking and trigger a range of responses in recipient cells [2,11]. For instance, hepatocyte-derived ApoBDs can improve hepatic stellate cell survival via JAK/STAT-mediated upregulation of anti-apoptotic protein Mcl-1 and stress-related activation of pro-survival PI3K/Akt/NF-κB cascade [12]. In a zebrafish model, basal stem cells were demonstrated to engulf ApoBDs released by neighbouring apoptotic stem cells, resulting in their Wnt8a-mediated cell division that is crucial to sustain tissue-wide cell number and epithelial homeostasis [13]. Under pathological conditions, such as cancer and infection, ApoBDs reportedly contain tumour and pathogen-derived antigens that can be recognised by the immune system, effectively leading to activation of adaptive immunity [14–18]. These findings not only uncover the key physiological and immunological roles of ApoBDs but also highlight the potential of ApoBD-based therapies and drug delivery system. Nevertheless, the therapeutic applications of ApoBDs remain poorly explored, which is largely attributed to limited insights into mechanisms of ApoBD biogenesis. In particular, as ApoBD cargoes have major influence on their functionality, improved understanding of the biology underlying the packaging and transferring of biomolecule cargos (e.g. nucleic acids, pathogen antigens, small molecule drugs) is key in harnessing their therapeutic potential.

In our previous report on cellular contents of ApoBDs, we noticed the elevated levels of DNA-containing vesicles through trovafloxacin-promoted ApoBD formation in apoptotic human Jurkat T cells [19]. Trovafloxacin, a quinolone-based antibiotic, was reportedly linked to serious adverse effects clinically, likely via recently-discovered PANX1 inhibition [1,20,21]. Of note, PANX1 belongs to a four-pass ATP-effluxing transmembrane channel family (PANX1–3), among which PANX1 is the

most widely expressed and implicated in regulating multiple biological and pathological processes [22]. Intriguingly, independently of its ATP release, PANX1 reportedly influences the content and plasticity of synaptic vesicles [23,24]. In fact, PANX1$^{-/-}$ mice display an altered distribution of vesicle-associated synaptic proteins [24]**.** Here, we therefore hypothesised that PANX1 would be an important regulator of nuclear cargo sorting into ApoBDs, which can be pharmacologically manipulatable using PANX1 inhibitors. To this end, using a differential centrifugation-based method [10], we purified ApoBDs for proteomic analysis, which revealed a pronounced enrichment of nuclear proteins in trovafloxacin-treated, apoptotic Jurkat T cell-derived ApoBDs. Furthermore, ApoBDs generated from PANX1 deficient (PANX1$^{-/-}$) cells displayed similar increased abundance of nuclear proteins as well as proportion of ApoBDs containing DNA. In addition, PANX1-interference, either by trovafloxacin or genetic disruption, also resulted in the formation of ApoBDs that are slightly smaller in size. These data presented in this study not only substantially extend our previous observation [19] but also thoroughly uncover the novel PANX1-mediated regulation of ApoBD size as well as nuclear content packaging. Significantly, this study may offer a new approach to pharmacologically manipulate this process using PANX1 inhibitors for ApoBD-based therapies.

2. Materials and methods

2.1. Reagents

Trovafloxacin (Trova), dimethyl sulfoxide (DMSO), Hoechst 33342 solution and poly-L-lysine solution were purchased from Sigma-Aldrich (MO). Other reagents were obtained as follows: annexin A5–phycoerythrin (A5-PE), 10× A5 binding buffer (BD Biosciences, CA) and TO-PRO-3 iodide (Life Technologies, NY).

2.2. Mammalian cell culture

Human Jurkat T cells were cultured in RPMI 1640 medium, supplemented with 10% fetal bovine serum, penicillin (50 U/ml), streptomycin (50 µg/ml) and MycoZap (Lonza, Switzerland) at 37 °C in a humidified atmosphere with 5% CO_2.

2.3. Induction of apoptosis

To induce apoptosis, Jurkat T cells at 1.5×10^6 cells/mL in serum-free RMPI 1640 supplemented with 1% BSA were treated with ultraviolet irradiation at 150 mJ/cm^2 using the Stratagene UV Stratalinker 1,800 (Agilent Technologies, CA). Subsequently, DMSO (0.2% v/v) or trovafloxacin (40 µM) were added and cell samples were incubated at 37 °C in a humidified atmosphere with 5% CO_2 for 4 h.

2.4. Purification of ApoBDs

ApoBDs were purified from UV-irradiated cell samples using differential centrifugation as previously described [9,10]. In brief, at 4 h post-UV, apoptotic cell samples were spun at 300 × *g* for 10 min to

remove cells (i.e. the 'whole apoptotic cell' fraction). The supernatant was then centrifuged at 3,000 × *g* for 20 min to separate ApoBDs (as pellet) from smaller EVs.

2.5. Flow cytometry analysis

Purified ApoBDs were stained with A5-PE (1:2,000), 0.2 μM TOPRO-3 and Hoescht 33342 (5 μg/mL) in 1× A5 binding buffer at room temperature for 10 min and immediately placed on ice before analysis using a BD FACSCanto II flow cytometer and FACSDiva 6.1.1 software (BD Bioscience). Unstained and single stained samples were used as a control and for spectral compensation. Data were analysed using FlowJo 10.7.1 software (Tree Star) as previously described [25].

2.6. Confocal microscopy

A5-PE and Hoescht 33342-stained ApoBDs were seeded onto a poly-L-lysine-coated Lab-Tek II chamber slide (Sigma-Aldrich). Samples were allowed to settle for 10 min prior to imaging using a LSM800 laser scanning confocal microscope (Zeiss, Germany).

2.7. In-gel digestion

Equal amount (30 μg) of protein samples (three biological replicates for each treatment) were separated in SDS-PAGE. The separated protein bands were visualized using Coomassie Brilliant Blue stain and the gel bands were then extracted using scalpel blades in to five gel bands. The bands were then reduced, alkylated and trypsinised as previously described [26]. Briefly, 10 mM DTT (Bio-Red) was used for reduction, 25 mM iodoacetamide (Sigma) was used for alkylation and the samples were trypsinized using 150 ng of trypsin (Promega). The tryptic peptides were extracted using 50% (w/v) acetonitrile and 0.1% (v/v) trifluroacetic acid.

2.8. LC-MS/MS

LC-MS/MS was carried out using the Fusion Lumos Orbitrap mass spectrometers (Thermo Fisher, USA). The LC system was equipped with an Acclaim Pepmap nano-trap column (Dinoex-C18, 100 Å, 75 μm x 2 cm) and an Acclaim Pepmap RSLC analytical column (Dinoex-C18, 100 Å, 75 μm x 50 cm). The tryptic peptides were injected into the enrichment column at an isocratic flow of 5 μL/min of 2% v/v acetonitrile containing 0.1% v/v formic acid for 6 min, applied before the enrichment column was switched in-line with the analytical column. The eluents were 0.1% v/v formic acid (solvent A) in water and 100% v/v acetonitrile in 0.1% v/v formic acid (solvent B). The flow gradient was (i) 0-6 min at 3% B; (ii) 6-35 min, 3-22% B; (iii) 35-40 min, 22-40% B; (iv) 45-50 min, 40-80% B; (v) 50-55 min, 80-80% B; (vi) 55-56 min 85-3% and equilibrated at 3% B for 10 min before injecting the next sample. The Fusion Lumos mass spectrometer was operated at positive-ionisation mode, with the spray voltage set at 1.9 kV and the ion transfer capillary temperature at 275 °C. The mass spectrometer was operated in the data-dependent acquisition mode, whereby full MS1 spectra were acquired in a positive mode at 120,000 resolution at m/z 200, with an AGC target of $5e^5$. The "top speed" acquisition mode (cycle time: 3 seconds) on the most intense precursor ion was used, whereby ions

with charge states of 2 to 5 were isolated using an isolation window of 1.2 m/z and fragmented with using HCD with a stepped collision energy of 30 ± 5%. Fragment ion spectra were acquired in Orbitrap at 15,000 resolution at m/z 200. Dynamic exclusion was 30 seconds.

Raw files were analysed using MaxQuant platform (version 1.6.17.0) [27] and searched against UniProt human database (20,394 reviewed Jan 2021) using default LFQ search parameters with the following parameters: LFQ min. ratio count = 2 with unique + razor peptides used for quantitation. Match between runs feature is activated. For this search Trypsin/P cleavage specificity (cleaves after lysine or arginine, even when proline is present) was used with a maximum of 2 missed cleavages. Oxidation of Methionine and Acetylation of protein N-Term were specified as variable modifications. Carbamidomethylation of cysteine was set as a fixed modification. False discovery rates (FDR) were determined through the target-decoy approach set to 1% for both peptides and proteins. LFQ intensities imported from the proteinGroups.txt output was Log2 transformed. The mass spectrometry proteomics data have been deposited to the ProteomeXchange Consortium via the PRIDE partner [28] repository with the dataset identifier PXD023988

2.9. Immunoblotting

Purified ApoBDs were lysed at 4°C using ice-cold lysis buffer (20 mM HEPES pH 7.4, 1% IGEPAL® CA-630, 10% glycerol, 1% Triton X-100, 150 mM NaCl, 50 mM NaF, protease inhibitor cocktail tablet; Sigma-Aldrich) with periodic vigorous agitation for 45 min. Protein concentration of the ApoBD lysates was determined using bicinchoninic acid assay. Subsequently, 30 µg of total protein per sample was subjected to reducing and denaturing SDS-PAGE prior to Western transfer onto nitrocellulose membrane (Bio-Rad). After blocking with 5% skim milk in PBS containing 0.1% (v/v) Tween®-20 (PBST), the membrane was probed with antibodies as followed: anti-human NUP50 (1:2,000), anti-human THYN1 (1:1,000), anti-human HMGA1 (1:10,000), anti-human PANX1 (1:1,000), anti-human β-actin (1:1,000) (all rabbit antibodies from Abcam) and horseradish peroxidase-conjugated donkey-anti-rabbit IgG (1:10,000; Cell Signaling Technology) in PBST containing 1% (w/v) BSA. Chemiluminescence detection was achieved using ECL Primer reagents (GE Healthcare, UK). Chemiluminescence signal intensity for protein bands was quantitated by densitometry analysis using ImageJ (National Institutes of Health, Bethesda, MD; http://imagej.nih.gov/ij/) and normalised against β-actin (loading control).

2.10. Cas9-CRISPR gene editing

PANX1$^{-/-}$ Jurkat T cells were previously generated using a doxycycline-inducible CRISPR/Cas9 system [29] and characterised in our recent study [6].

2.11. Statistical analyses

Data represent mean ± SEM. Statistical significance was determined using one-way ANOVA with a Tukey post-hoc test or Student's t-test where appropriate. A *p*-value of <0.05 was considered

statistically significant. Sample size and number of replicates are specified within the figure legends. FunRich analysis tool - version 3.1.3 [30] was used to generate the Venn diagrams and heatmaps.

3. Results and discussion

Previous studies showed that genetic disruption of the membrane channel PANX1 in mice resulted in the modification of synaptic vesicle content [24]. We also observed that trovafloxacin, a PANX1 inhibitor, not only promotes ApoBD formation but also increases the proportion of ApoBDs containing DNA [19]. Therefore, we asked whether PANX1, apart from being a negative regulator of the membrane protrusion step of apoptotic cell disassembly, also governs nuclear cargo sorting into ApoBDs. To address this question initially using a pharmacologic approach, we isolated ApoBDs from the UV-induced apoptotic Jurkat T cells in the absence or presence of DMSO (*untreated* and *vehicle control*, respectively) or 40 µM trovafloxacin (**Figure 1a**), using a differential centrifugation approach [10]. Consistent with previous studies, the isolated ApoBDs (post-3,000 x *g* pellets) in all three conditions were of high purity (>96%) and stained positively for annexin A5 (A5), indicative of phosphatidylserine exposure on the EVs (an ApoBD marker) (**Figure 1b**). Confocal imaging confirmed the A5 staining, whilst Hoechst staining indicated the presence of DNA cargos in some ApoBDs (**Figure 1c**). Notably, isolated ApoBDs also contained cleaved caspase substrate, cleaved PANX1 (**Figure 1d**), an ApoBD marker described previously [31]. Interestingly, though the majority of isolated ApoBD were within the traditional size range of 1–5 µm (**Figure 1e**) and consistent with confocal microscopy data, ApoBDs derived from trovafloxacin treatments (average size of 3.7 µm) were slightly, but significantly, smaller than those from untreated control and vehicle control samples (~4.1 µm). These quality control data together confirmed the identity, purity and quality, thus suitability of ApoBD preparation from all three conditions for subsequent proteomic analyses.

The proteomic profiling uncovers the pronounced difference in protein contents in trovafloxacin-derived ApoBDs, compared to the untreated and vehicle controls (**Figure 2a**). Furthermore, the cellular component gene ontology (GO) analysis intriguingly revealed the significant abundance of nuclear proteins upon trovafloxacin treatment (**Figure 2b**). These enrichment patterns were not mirrored in the whole apoptotic cells (post-300 x *g* pellets) proteomes (**Figure 2c**), suggesting that trovafloxacin specifically affects the nuclear protein sorting into ApoBDs. This trovafloxacin-induced nuclear protein enrichment is further exemplified in the heatmap (**Figure 2d**). To experimentally verify this proteomic observation, using immunoblotting (**Figure 2e**), we were able detect presentative nuclear proteins clearly evidently elevated in trovafloxacin-treated ApoBD samples, namely high mobility group protein A1 (HMGA1, *a dsDNA-binding nucleosome resident* [32]), thymocyte nuclear protein 1 (THYN1, *localised in nucleoplasm and associated with apoptosis induction* [33]) and 50 kD nucleoporin (NUP50, *nuclear pore complex protein* [34]). Their nuclear origin diversity may indicate that nuclear protein transport is unlikely to be a mere concomitant event of DNA packaging.

Next, we sought to define the involvement of PANX1 in the sorting of nuclear cargoes (DNA and proteins) into ApoBDs by a genetic approach. To this end, we harvested ApoBDs from UV-induced apoptotic PANX1$^{-/-}$ Jurkat T cells (generated previously by CRISPR/Cas9 gene editing [6]) and Cas9 expressing Jurkat T cells as a control. Consistently, the isolated ApoBDs in both cell lines were A5^{+} and of high purity (~97%, **Figure 3a**). A5 staining and presence of DNA cargos were visualised by confocal imaging (**Figure 3b**). PANX1$^{-/-}$-derived ApoBDs, as expected, is absent of full-length and cleaved PANX1 as compared to the Cas9 counterparts (**Figure 3c**). Importantly, like trovafloxacin treatment, apoptotic PANX1$^{-/-}$ Jurkat T cells also generated ApoBDs that are smaller (on average 3.6 µm, as comparted to 4.1 µm for Cas9 Jurkat-derived ApoBDs; **Figure 3d**), significantly increased abundance of nuclear proteins such as HMGA1, THYN1 and NUP50 (**Figure 3e**), as well as elevated DNA level as indicated by flow cytometry using DNA-detecting Hoechst stain (**Figure 3f**). Collectively, these data suggest that PANX1 regulates the distribution of nuclear content in ApoBDs negatively as well as modulates the size of ApoBDs.

During apoptotic cell disassembly, a fundamental process downstream of apoptosis, PANX1 activity is activated by caspase 3/7 cleavage during apoptosis [35] and can limit the generation of thin apoptotic protrusions called apoptopodia, which in turn restrain detachment of blebs from the apoptotic cells to form distinct ApoBDs [1]. Targeting PANX1, either by pharmacological blockade or genetic disruption substantially enhanced apoptopodia formation and consequently ApoBD generation [1]. Intriguingly, our study identifies PANX1 as a negative regulator of ApoBD nuclear protein packaging as well as a modulator of ApoBD size. Our findings add another level of complexity and multifunctionality of PANX1 that underpins many critical physiological and pathological processes, including apoptotic cell disassembly and clearance [1,22]. It remains unknown how PANX1 controls ApoBD contents, which is nonetheless unlikely mediated by its conventional ATP release activity as extracellular ATP does not influence the ApoBD formation process [1]. Alternatively, the simultaneous sorting of DNA and proteins of diverse nuclear origin (*e.g.* nucleosomes, nucleoplasm and nuclear envelope) may hint that PANX1 could modify the packaging of apoptosis-induced nuclear fragments, possibly via its ca permeation effect [36]. During apoptosis, nuclear fragmentation is mediated by caspase cleavage-mediated breakdown of calcium-sensitive lamins, nuclear architectural proteins [37–39]. As PANX1 channel opens upon caspase cleavage, the resulting increased calcium inside the apoptotic cells can promote further lamin degradation [39] and hence nuclear fragmentation into smaller fragments that in turn enter ApoBDs more easily.

Importantly, our demonstrations of PANX1 involvement in nuclear cargo sorting and its druggability may have opened up a new avenue to clinically adopting ApoBD-based therapies, particularly vaccines and therapeutic loading. Reportedly, tumour-derived antigens contained in ApoBDs can be immunologically recognised and processed by ApoBD-engulfing professional antigen-presenting cells (APCs; *e.g.* dendritic cells, macrophages) to promote adaptive immune responses. In fact, a few studies have claimed the effectiveness of tumour ApoBD-efferocytosed antigen-presenting cells in triggering antitumour responses and reducing disease burdens in preclinical mouse models and human patients [15–18]. Promisingly, ApoBDs have two unique properties that may offer less off-target effect and potent response over healthy cell-derived EVs and other antigen-pulsing

approaches: (i) the specific molecular machinery for ApoBD recognition and efferocytosis by APCs, and (ii) more efficient generation of MHC-antigen complex compared to pre-processed peptides and tumour cell-APC hybrid [40,41]. In these particular settings, by pharmacologically targeting PANX1 using inhibitors such as trovafloxacin during the production of these tumour nuclear antigens encapsulated ApoBDs, the quantity (through enhancing ApoBD production) and quality (through elevated nuclear antigen sorting) may be improved. Using similar approach, as ApoBDs hold potential as a drug delivery system [3], therapeutic nuclear proteins, such as nuclear resident transcription factors [42], could be efficiently loaded onto ApoBDs by engineering them into host cells followed by apoptosis induction and PANX1 inhibitor treatments.

4. Conclusion

It is becoming clear that ApoBDs are more than 'garbage bags' for disposal of dying cells' materials. With recent mechanistic and functional findings, ApoBDs are emerging as a therapeutically exploitable EV subtype. ApoBDs' unique link to cell death and natural recognition by phagocytes provide distinctive opportunities for future therapeutic design as vaccine, immunotherapies, drug delivery and disease diagnosis. Therefore, better understanding of ApoBD biology as well as developing novel approaches to engineer and/or modify ApoBDs, such as our findings on novel role and pharmacological manipulation of PANX1-regulated nuclear content sorting herein, could be beneficial in achieving desired therapeutic responses.

Author contributions

The study was conceived, designed and supervised by T.K.P, S.M. and I.K.H.P. T.K.P. and P.F equally performed experiments. R.T. generated PANX$^{-/-}$ Jurkat T cell line. M.P., C.S.A., D.C.O. contributed to experimental design and discussion. All authors analysed and interpreted the data. The manuscript was written by T.K.P., P.F, S.M. and I.K.H.P., reviewed and approved by all co-authors.

Acknowledgements

This work was funded by the National Health and Medical Research Council [GNT1125033, GNT1140187] and La Trobe University Research Focus Area.

Conflicts of interest

The authors declare that there is no conflict of interest

Figure legends

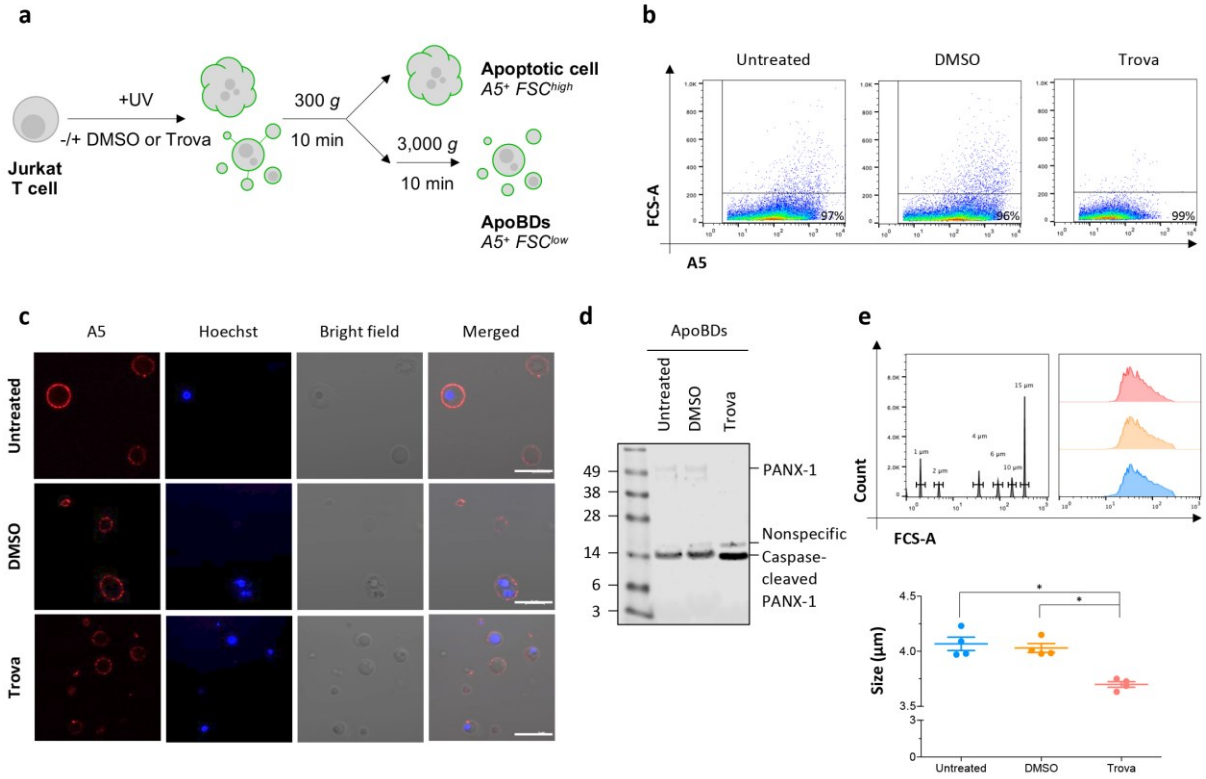

Figure 1. ApoBD purification and characterisation

a, Schematic for purifying ApoBDs from Jurkat T cells (untreated control, 0.2% DMSO vehicle control or 40 µM trovafloxacin (Trova)). **b,** Purity assessment by flow cytometry analysis according to previous studies [10,19]. **c,** Confocal imaging of purified ApoBDs. **d,** Detection of caspase-cleaved substrates, *e.g.* PANX1, as ApoBD markers by immunoblotting. Loading controls (β-actin) are same as figure 2e. Data are representative of at least 3 independent experiments. Scale bars are 10 µm. **e,** ApoBD sizing (n=4). * denotes p-value of <0.05 and ** denotes p<0.01 as determined by one-way ANOVA with a Tukey post-hoc test.

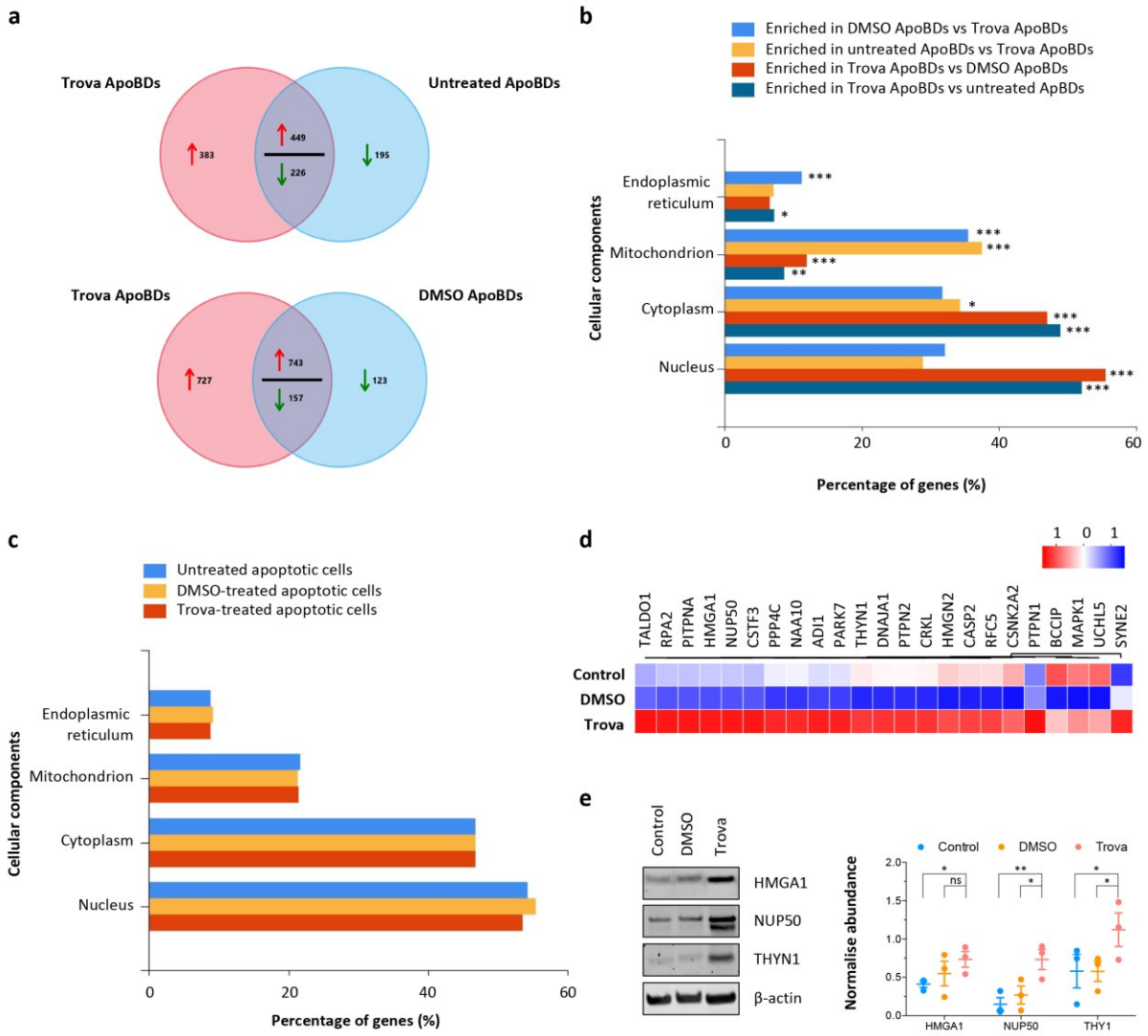

Figure 2. Trovafloxacin induces enrichment of nuclear proteins packaged in ApoBDs

a, Venn diagrams for differentially abundant proteins and **b,** Cellular component GO analysis of proteins enriched in ApoBDs derived from trovafloxacin treatment compared to untreated and DSMO control (n=3). Proteins enriched (2-fold and above) were compared against FunRich database. **c,** Cellular component GO analysis for whole apoptotic cell proteomes (n=3). **(d)** Heatmap of representative nuclear proteins in ApoBDs under different conditions. **e,** Immunoblotting analysis comparing abundance of nuclear proteins in ApoBDs (n=3). * denotes p-value of <0.05 and ** denotes p<0.01 as determined by Student's t-test or one-way ANOVA with a Tukey post-hoc test.

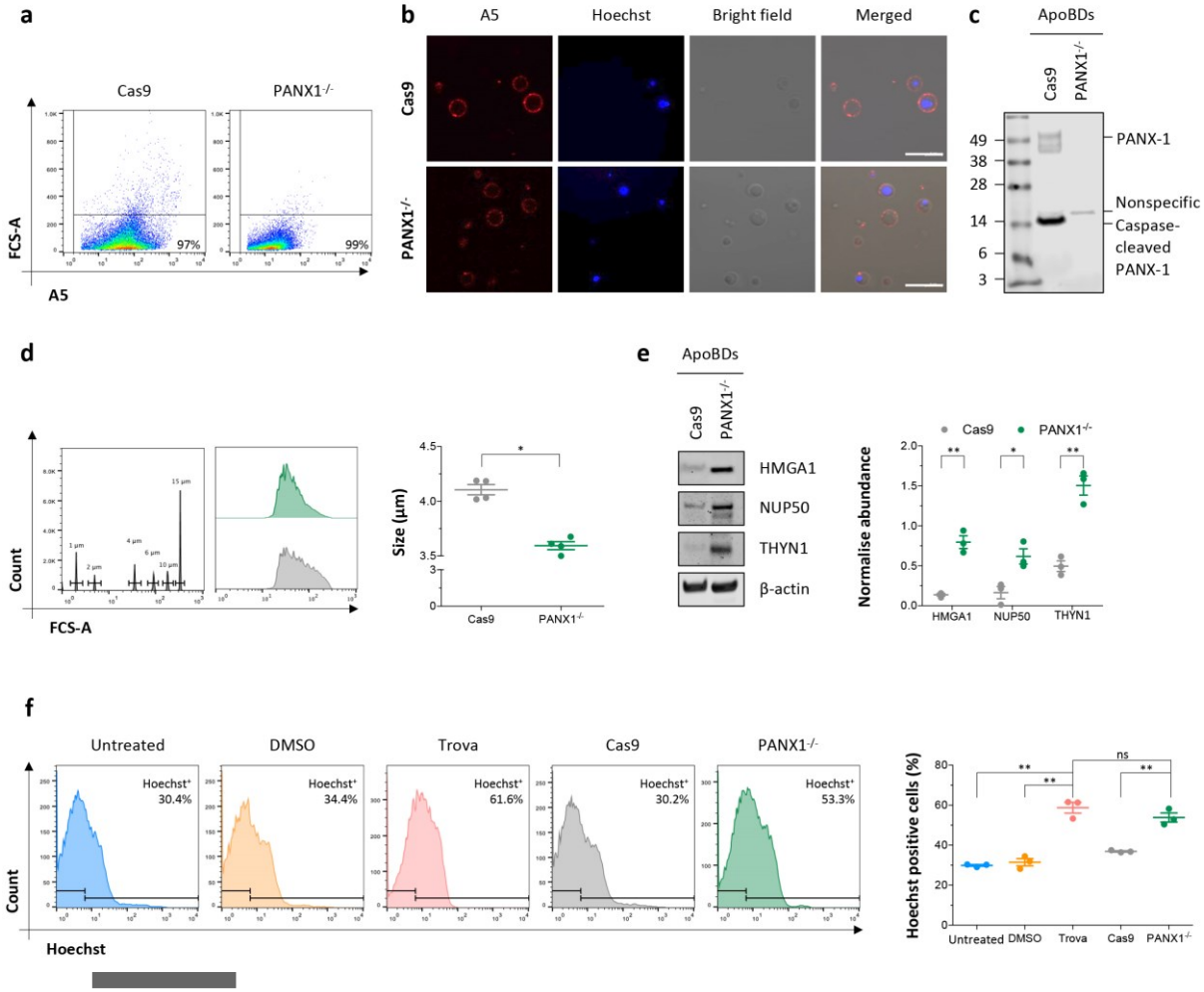

Figure 3. Genetic disruption of PANX1 channel increases packaging of nuclear contents into ApoBDs

a, Purity assessment of ApoBD preparation from Cas9 and PANX1$^{-/-}$ Jurkat T cells by flow cytometry analysis. **b,** Confocal imaging of purified ApoBDs. Data are representative of at least 3 independent experiments. Scale bars are 10 µm. **c,** Confirmation of PANX1 disruption in the purified ApoBDs. Loading controls (β-actin) are same as figure 3e. **d,** ApoBD sizing (n=4). **e,** Immunoblotting analysis comparing abundance of nuclear proteins in ApoBDs (n=3). **f,** Flow cytometry analysis showing the DNA contents in ApoBDs based on Hoechst staining (n=3). * denotes p-value of <0.05 and ** denotes p<0.01 as determined by Student's t-test or one-way ANOVA with a Tukey post-hoc.

References

[1] I.K. Poon, Y.H. Chiu, A.J. Armstrong, J.M. Kinchen, I.J. Juncadella, D.A. Bayliss, K.S. Ravichandran, Unexpected link between an antibiotic, pannexin channels and apoptosis, Nature. 507 (2014) 329–334. https://doi.org/10.1038/nature13147.

[2] G.K. Atkin-Smith, I.K.H. Poon, Disassembly of the Dying: Mechanisms and Functions, Trends Cell Biol. 27 (2017) 151–162. https://doi.org/10.1016/j.tcb.2016.08.011.

[3] T.K. Phan, D.C. Ozkocak, I.K.H. Poon, Unleashing the therapeutic potential of apoptotic bodies, Biochem. Soc. Trans. (2020). https://doi.org/10.1042/BST20200225.

[4] M.L. Coleman, E.A. Sahai, M. Yeo, M. Bosch, A. Dewar, M.F. Olson, Membrane blebbing during apoptosis results from caspase-mediated activation of ROCK I, Nat. Cell Biol. (2001). https://doi.org/10.1038/35070009.

[5] M. Sebbagh, C. Renvoizé, J. Hamelin, N. Riché, J. Bertoglio, J. Bréard, Caspase-3-mediated cleavage of ROCK I induces MLC phosphorylation and apoptotic membrane blebbing, Nat. Cell Biol. (2001). https://doi.org/10.1038/35070019.

[6] R. Tixeira, T.K. Phan, S. Caruso, B. Shi, G.K. Atkin-Smith, C. Nedeva, J.D.Y. Chow, H. Puthalakath, M.D. Hulett, M.J. Herold, I.K.H. Poon, ROCK1 but not LIMK1 or PAK2 is a key regulator of apoptotic membrane blebbing and cell disassembly, Cell Death Differ. 27 (2020). https://doi.org/10.1038/s41418-019-0342-5.

[7] G.K. Atkin-Smith, M.A. Miles, R. Tixeira, F.T. Lay, M. Duan, C.J. Hawkins, T.K. Phan, S. Paone, S. Mathivanan, M.D. Hulett, W. Chen, I.K.H. Poon, Plexin B2 Is a Regulator of Monocyte Apoptotic Cell Disassembly, Cell Rep. 29 (2019) 1821–1831. https://doi.org/10.1016/j.celrep.2019.10.014.

[8] D.K. Moss, V.M. Betin, S.D. Malesinski, J.D. Lane, A novel role for microtubules in apoptotic chromatin dynamics and cellular fragmentation, J Cell Sci. 119 (2006) 2362–2374. https://doi.org/10.1242/jcs.02959.

[9] G.K. Atkin-Smith, S. Paone, D.J. Zanker, M. Duan, T.K. Phan, W. Chen, M.D. Hulett, I.K.H. Poon, Isolation of cell type-specific apoptotic bodies by fluorescence-activated cell sorting, Sci. Rep. 7 (2017). https://doi.org/10.1038/srep39846.

[10] T.K. Phan, I.K.H. Poon, G.K. Atkin-Smith, Detection and isolation of apoptotic bodies to high purity, J. Vis. Exp. 2018 (2018). https://doi.org/10.3791/58317.

[11] X. Xu, Y. Lai, Z.C. Hua, Apoptosis and apoptotic body: Disease message and therapeutic target potentials, Biosci. Rep. (2019). https://doi.org/10.1042/BSR20180992.

[12] J.X. Jiang, K. Mikami, S. Venugopal, Y. Li, N.J. Török, Apoptotic body engulfment by hepatic stellate cells promotes their survival by the JAK/STAT and Akt/NF-κB-dependent pathways, J. Hepatol. (2009). https://doi.org/10.1016/j.jhep.2009.03.024.

[13] C.K. Brock, S.T. Wallin, O.E. Ruiz, K.M. Samms, A. Mandal, E.A. Sumner, G.T. Eisenhoffer, Stem cell proliferation is induced by apoptotic bodies from dying cells during epithelial tissue maintenance, Nat. Commun. (2019). https://doi.org/10.1038/s41467-019-09010-6.

[14] U.E. Schaible, F. Winau, P.A. Sieling, K. Fischer, H.L. Collins, K. Hagens, R.L. Modlin, V. Brinkmann, S.H.E. Kaufmann, Apoptosis facilitates antigen presentation to T lymphocytes through MHC-I and CD1 in tuberculosis, Nat. Med. (2003). https://doi.org/10.1038/nm906.

[15] F. Henry, O. Boisteau, L. Bretaudeau, B. Lieubeau, K. Meflah, M. Grégoire, Antigen-presenting cells that phagocytose apoptotic tumor-derived cells are potent tumor vaccines, Cancer Res. (1999).

[16] P. Kokhaei, M.R. Rezvany, L. Virving, A. Choudhury, H. Rabbani, A. Österborg, H. Mellstedt, Dendritic cells loaded with apoptotic tumour cells induce a stronger T-cell response than dendritic cell-tumour hybrids in B-CLL, Leukemia. (2003). https://doi.org/10.1038/sj.leu.2402913.

[17] M. Palma, L. Hansson, A. Choudhury, B. Näsman-Glaser, I. Eriksson, L. Adamson, E. Rossmann, K. Widén, R. Horváth, P. Kokhaei, S. Vertuani, H. Mellstedt, A. Österborg, Vaccination with dendritic cells loaded with tumor apoptotic bodies (Apo-DC) in patients with chronic lymphocytic leukemia: Effects of various adjuvants and definition of immune response criteria, Cancer Immunol. Immunother. (2012). https://doi.org/10.1007/s00262-011-1149-5.

[18] I. Hus, J. Roliński, J. Tabarkiewicz, K. Wojas, A. Bojarska-Junak, J. Greiner, K. Giannopoulos, A. Dmoszyńska, M. Schmitt, Allogeneic dendritic cells pulsed with tumor lysates or apoptotic bodies as immunotherapy for patients with early-stage B-cell chronic lymphocytic leukemia, Leukemia. (2005). https://doi.org/10.1038/sj.leu.2403860.

[19] L. Jiang, S. Paone, S. Caruso, G.K. Atkin-Smith, T.K. Phan, M.D. Hulett, I.K.H. Poon, Determining the contents and cell origins of apoptotic bodies by flow cytometry, Sci. Rep. 7 (2017). https://doi.org/10.1038/s41598-017-14305-z.

[20] G. Giustarini, N. Vrisekoop, L. Kruijssen, L. Wagenaar, S. Van Staveren, M. Van Roest, R. Bleumink, M. Bol-Schoenmakers, R.J. Weaver, L. Koenderman, J. Smit, R. Pieters, Trovafloxacin-Induced Liver Injury: Lack in Regulation of Inflammation by Inhibition of Nucleotide Release and Neutrophil Movement, Toxicol. Sci. (2019). https://doi.org/10.1093/toxsci/kfy244.

[21] C. Garg, J.H. Seo, J. Ramachandran, J.M. Loh, F. Calderon, J.E. Contreras, Trovafloxacin attenuates neuroinflammation and improves outcome after traumatic brain injury in mice, J. Neuroinflammation. (2018). https://doi.org/10.1186/s12974-018-1069-9.

[22] Y.H. Chiu, M.S. Schappe, B.N. Desai, D.A. Bayliss, Revisiting multimodal activation and channel properties of Pannexin 1, J. Gen. Physiol. (2018). https://doi.org/10.1085/jgp.201711888.

[23] J.C. Sanchez-Arias, M. Liu, C.S.W. Choi, S.N. Ebert, C.E. Brown, L.A. Swayne, Pannexin 1 regulates network ensembles and dendritic spine development in cortical neurons, ENeuro. (2019). https://doi.org/10.1523/ENEURO.0503-18.2019.

[24] I. Gajardo, C.S. Salazar, D. Lopez-Espíndola, C. Estay, C. Flores-Muñoz, C. Elgueta, A.M. Gonzalez-Jamett, A.D. Martínez, P. Muñoz, Á.O. Ardiles, Lack of pannexin 1 alters synaptic GluN2 subunit composition and spatial reversal learning in mice, Front. Mol. Neurosci. (2018). https://doi.org/10.3389/fnmol.2018.00114.

[25] L. Jiang, R. Tixeira, S. Caruso, G.K. Aktin-Smith, A.A. Baxter, M.D. Hulett, S. Paone, I.K. Poon, Monitoring the progression of cell death and disassembly of dying cells by flow cytometry, Nat. Protoc. 4 (2016) 655–663.

[26] P. Fonseka, M. Liem, C. Ozcitti, C.G. Adda, C.S. Ang, S. Mathivanan, Exosomes from N-Myc amplified neuroblastoma cells induce migration and confer chemoresistance to non-N-Myc amplified cells: implications of intra-tumour heterogeneity, J. Extracell. Vesicles. (2019). https://doi.org/10.1080/20013078.2019.1597614.

[27] J. Cox, M. Mann, MaxQuant enables high peptide identification rates, individualized p.p.b.-range mass accuracies and proteome-wide protein quantification, Nat. Biotechnol. (2008). https://doi.org/10.1038/nbt.1511.

[28] Y. Perez-Riverol, A. Csordas, J. Bai, M. Bernal-Llinares, S. Hewapathirana, D.J. Kundu, A. Inuganti, J. Griss, G. Mayer, M. Eisenacher, E. Pérez, J. Uszkoreit, J. Pfeuffer, T. Sachsenberg, Ş. Yilmaz, S. Tiwary, J. Cox, E. Audain, M. Walzer, A.F. Jarnuczak, T. Ternent, A. Brazma, J.A. Vizcaíno, The PRIDE database and related tools and resources in 2019: Improving support for quantification data, Nucleic Acids Res. (2019). https://doi.org/10.1093/nar/gky1106.

[29] A.J. Kueh, M.J. Herold, Using CRISPR/Cas9 Technology for Manipulating Cell Death Regulators, (2016) 253–264. https://doi.org/10.1007/978-1-4939-3581-9_18.

[30] M. Pathan, S. Keerthikumar, C.S. Ang, L. Gangoda, C.Y.J. Quek, N.A. Williamson, D. Mouradov, O.M. Sieber, R.J. Simpson, A. Salim, A. Bacic, A.F. Hill, D.A. Stroud, M.T. Ryan, J.I. Agbinya, J.M. Mariadason, A.W. Burgess, S. Mathivanan, FunRich: An open access standalone functional enrichment and interaction network analysis tool, Proteomics. (2015). https://doi.org/10.1002/pmic.201400515.

[31] I.K.H. Poon, M.A.F. Parkes, L. Jiang, G.K. Atkin-Smith, R. Tixeira, C.D.C.D. Gregory, D.C. Ozkocak, S.F. Rutter, S. Caruso, J.P. Santavanond, S. Paone, B. Shi, A.L. Hodge, M.D. Hulett, J.D.Y. Chow, T.K. Phan, A.A. Baxter, Moving beyond size and phosphatidylserine exposure: evidence for a diversity of apoptotic cell-derived extracellular vesicles in vitro, J. Extracell. Vesicles. 8 (2019). https://doi.org/10.1080/20013078.2019.1608786.

[32] E. Chiefari, M.T. Nevolo, B. Arcidiacono, E. Maurizio, A. Nocera, S. Iiritano, R. Sgarra, K. Possidente, C. Palmieri, F. Paonessa, G. Brunetti, G. Manfioletti, D. Foti, A. Brunetti, HMGA1 is a novel downstream nuclear target of the insulin receptor signaling pathway, Sci. Rep. (2012). https://doi.org/10.1038/srep00251.

[33] X.Z. Jiang, H. Toyota, T. Yoshimoto, E. Takada, H. Asakura, J. Mizuguchi, Anti-IgM-induced down-regulation of nuclear Thy28 protein expression in Ramos B lymphoma cells, Apoptosis. (2003). https://doi.org/10.1023/A:1025594409056.

[34] M.E. Lindsay, K. Plafker, A.E. Smith, B.E. Clurman, I.G. Macara, Npap60/Nup50 is a tri-stable switch that stimulates importin-α:β-mediated nuclear protein import, Cell. (2002). https://doi.org/10.1016/S0092-8674(02)00836-X.

[35] J.K. Sandilos, Y.H. Chiu, F.B. Chekeni, A.J. Armstrong, S.F. Walk, K.S. Ravichandran, D.A. Bayliss, Pannexin 1, an ATP release channel, is activated by caspase cleavage of its pore-associated C-terminal autoinhibitory region, J. Biol. Chem. (2012). https://doi.org/10.1074/jbc.M111.323378.

[36] Y.H. Chiu, X. Jin, C.B. Medina, S.A. Leonhardt, V. Kiessling, B.C. Bennett, S. Shu, L.K. Tamm, M. Yeager, K.S. Ravichandran, D.A. Bayliss, A quantized mechanism for activation of pannexin channels, Nat. Commun. (2017). https://doi.org/10.1038/ncomms14324.

[37] C.Y. Ho, J. Lammerding, Lamins at a glance, J. Cell Sci. (2012). https://doi.org/10.1242/jcs.087288.

[38] L. Rao, D. Perez, E. White, Lamin proteolysis facilitates nuclear events during apoptosis, J. Cell Biol. (1996). https://doi.org/10.1083/jcb.135.6.1441.

[39] N. Neamati, A. Fernandez, S. Wright, J. Kiefer, D.J. McConkey, Degradation of lamin B1 precedes oligonucleosomal DNA fragmentation in apoptotic thymocytes and isolated thymocyte nuclei, J. Immunol. (1995).

[40] I.K.H. Poon, C.D. Lucas, A.G. Rossi, K.S. Ravichandran, Apoptotic cell clearance: Basic biology and therapeutic potential, Nat. Rev. Immunol. (2014). https://doi.org/10.1038/nri3607.

[41] K. Inaba, S. Turley, F. Yamaide, T. Iyoda, K. Mahnke, M. Inaba, M. Pack, M. Subklewe, B. Sauter, D. Sheff, M. Albert, N. Bhardwaj, I. Mellman, R.M. Steinman, Efficient presentation of phagocytosed cellular fragments on the major histocompatibility complex class II products of dendritic cells, J. Exp. Med. (1998). https://doi.org/10.1084/jem.188.11.2163.

[42] C. Bichsel, D.K. Neeld, T. Hamazaki, D. Wu, L.J. Chang, L. Yang, N. Terada, S. Jin, Bacterial delivery of nuclear proteins into pluripotent and differentiated cells, PLoS One. (2011). https://doi.org/10.1371/journal.pone.0016465.